

Circular band formation for incompressible viscous fluid–rigid particle mixtures in a rotating cylinder

Suchung Hou¹, Tsorng-Whay Pan^{2,*} and Roland Glowinski²

¹Department of Mathematics, National Cheng Kung University, Tainan 701, Taiwan, R.O.C.

²Department of Mathematics, University of Houston, Houston, TX 77204, USA

Abstract

In this paper we have investigated a circular band formation of fluid-rigid particle mixtures in a fully filled cylinder horizontally rotating about its cylinder axis by direct numerical simulation. These phenomena are modeled by the Navier-Stokes equations coupled to the Euler-Newton equations describing the rigid solid motion of the non-neutrally particles. The formation of circular bands studied in this paper is not resulted by mutual interaction between the particles and the periodic inertial waves in the cylinder axis direction (as suggested in Phys. Rev. E, 72, 021407 (2005)), but due to the interaction of particles. When a circular band is forming, the part of the band formed by the particles moving downward becomes more compact due to the particle interaction strengthened by the downward acceleration from the gravity. The part of a band formed by the particles moving upward is always loosening up due to the slow down of the particle motion by the counter effect of the gravity. To form a compact circular band (not a loosely one), enough particles are needed to interact among themselves continuously through the entire circular band at a rotating rate so that the upward diffusion of particles can be balanced by the compactness process when these particles moving downward.

1 Introduction

Non-equilibrium systems often organize into interesting spatio-temporal structures or patterns. Examples include the patterns in pure fluid flow systems, such as the Taylor-Couette flow between two concentric rotating cylinders and well-defined periodic bands of particles in a partially or fully filled horizontally rotating cylinder. Particulate flows exhibiting circular bands in a partially filled horizontal rotating cylinder are in part attributed to the presence of the free surface caused by the partial filling of the cylinder (e.g., see [1, 2, 3]). In a fully filled horizontally rotating cylinder, band and other pattern formations were also found in the suspensions of non-Brownian settling particles in [4]-[10]. In this paper, we have focused on the understanding of the band formation closely related to those observed in [9, 10], which are different from those considered experimentally in [4, 5, 6, 7] and numerically in [11, 12]. The ratio of the particle diameter and the inner cylinder diameter in [9, 10] is about 6 to 7%, which is larger than the particles of the ratio of 1% used in [4, 5, 6, 7, 11, 12]. The cylinder rotating rate is in the range between 6 to 10 sec^{-1} in [9, 10] and the fluid-particle mixture is not in the Stoke flow regime as considered computationally in [11, 12]. In [8] Lipson used a horizontal rotating cylinder filled with over-saturated solution to grow crystal without any interaction with a substrate and found that crystals accumulate in well-defined periodic bands, normal to the axis of rotation. Lipson and Seiden [9] just suggested, with no further discussion, that it could be the interaction between particles and fluid in the tube. In [10], Seiden et al. did an experimental investigation of the dependence of the formation of bands on particle characteristics, tube diameter and length, and fluid viscosity. They suggested that the segregation of particles occurs as a result of mutual interaction between the particles and inertial waves excited in the bounded fluid. In [13] Seiden et al. believed that the axial pressure gradient associated with an inertial-mode excitation within bounded fluid is responsible for the formation of bands according to their general dimensionless analysis. A single ball motion was discussed by solving the equation of motion for the ball with a one-way coupling in a filled and horizontally rotating

*Corresponding author. E-mail address: pan@math.uh.edu

cylinder; a stability analysis and a phase diagram based on one ball motion are addressed; but they did not consider the effect of the ball to the fluid and the interaction among many particles.

Via the direct numerical simulations, we have found that, at least for all cases considered in this paper the formation of circular bands is not resulted by mutual interaction between the particles and the periodic inertial waves in the cylinder axis direction as suggested in [10, 13], but by the interaction between particles. In our simulations, the particles form a layer inside a horizontally rotating cylinder as in Figure 7 in [10]. These particles are partially coated on the inner wall of the rotating cylinder under the influence of a strong centrifugal force. When a circular band is forming, the part of the band formed by the particles moving downward becomes more compact due to the particle interaction strengthened by the downward acceleration from the gravity. The part of a band formed by the particles moving upward is always loosening up due to the slow down of the particle motion by the counter effect of the gravity. To form a compact circular band (not a loosely one), enough particles are needed to interact among themselves continuously through the entire circular band at a rotating rate so that the compactness of the whole circular band can be maintained when these particles moving upward. Hence the balance of the gravity, the rotating rate, and the fluid flow inertia plus enough number of particles is important on the formation of circular bands in a fully filled cylinder.

The scheme of this paper is as follows: We discuss the models and numerical methods briefly in Sec. 2. In Sec. 3, we study the effect of the particle number and rotating rate on the formation of circular bands and then present the flow field development under the influence of the particle interaction to show that the formation of circular bands studied in this paper is not resulted by the periodic inertial waves in the cylinder axis direction. The conclusions are summarized in Sec. 4.

2 Model and numerical method

To perform the *direct numerical simulation* of the interaction between rigid bodies and fluid, we have developed a methodology which combines a distributed Lagrange multiplier based fictitious domain method with operator splitting and finite element methods (e.g., see [14]-[19]). For a ball B moving in a Newtonian viscous incompressible fluid of the viscosity μ and the density ρ contained in a truncated cylinder \mathbf{C} under the effect of the gravity depicted in Figure 1, the flow is modeled by the Navier-Stokes equations, namely,

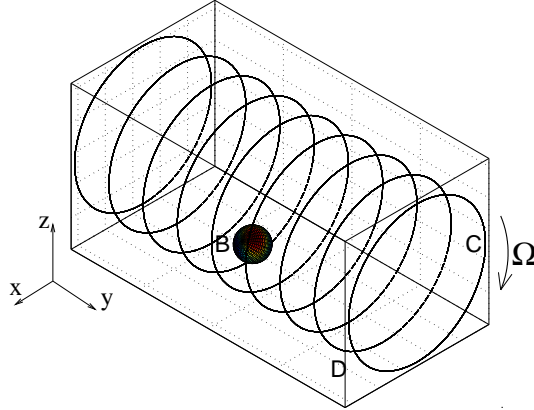


Figure 1: The flow region with a ball B in a truncated cylinder \mathbf{C} .

$$\rho \left[\frac{\partial \mathbf{u}}{\partial t} + (\mathbf{u} \cdot \nabla) \mathbf{u} \right] - \mu \Delta \mathbf{u} + \nabla p = \mathbf{g} \text{ in } \{(\mathbf{x}, t) | \mathbf{x} \in \mathbf{C} \setminus \overline{B(t)}, t \in (0, T)\}, \quad (1)$$

$$\nabla \cdot \mathbf{u}(t) = 0 \text{ in } \{(\mathbf{x}, t) | \mathbf{x} \in \mathbf{C} \setminus \overline{B(t)}, t \in (0, T)\}, \quad (2)$$

$$\mathbf{u}(0) = \mathbf{u}_0(\mathbf{x}), \text{ (with } \nabla \cdot \mathbf{u}_0 = 0), \quad (3)$$

$$\mathbf{u} = \mathbf{g}_0 \text{ on } \Gamma_0 \times (0, T), \text{ (with } \int_{\Gamma_0} \mathbf{g}_0 \cdot \mathbf{n} d\Gamma = 0), \quad (4)$$

where Γ_0 is the boundary of a truncated cylinder \mathbf{C} , \mathbf{g} denotes gravity and \mathbf{n} is the unit normal vector pointing outward to the flow region. We assume a *no-slip condition* on $\gamma(= \partial B)$. The motion of the rigid body B satisfies the Euler-Newton's equations, namely

$$\mathbf{v}(\mathbf{x}, t) = \mathbf{V}(t) + \vec{\omega}(t) \times \overrightarrow{\mathbf{G}(t)\mathbf{x}}, \quad \forall \mathbf{x} \in \overline{B(t)}, \quad \forall t \in (0, T), \quad (5)$$

$$\frac{d\mathbf{G}}{dt} = \mathbf{V}, \quad (6)$$

$$M_p \frac{d\mathbf{V}}{dt} = M_p \mathbf{g} + \mathbf{F}_H, \quad (7)$$

$$\mathbf{I}_p \frac{d\boldsymbol{\omega}}{dt} = \mathbf{T}_H, \quad (8)$$

with the resultant and torque of the hydrodynamical forces given by, respectively,

$$\mathbf{F}_H = - \int_{\gamma} \boldsymbol{\sigma} \mathbf{n} d\gamma, \quad \mathbf{T}_H = - \int_{\gamma} \overrightarrow{\mathbf{G}\mathbf{x}} \times \boldsymbol{\sigma} \mathbf{n} d\gamma \quad (9)$$

with $\boldsymbol{\sigma} = \mu(\nabla \mathbf{u} + \nabla \mathbf{u}^t) - p\mathbf{I}$. Equations (1)–(9) are completed by the following initial conditions

$$\mathbf{G}(0) = \mathbf{G}_0, \quad \mathbf{V}(0) = \mathbf{V}_0, \quad \boldsymbol{\omega}(0) = \boldsymbol{\omega}_0, \quad B(0) = B_0. \quad (10)$$

Above, M_p , \mathbf{I}_p , \mathbf{G} , \mathbf{V} and $\boldsymbol{\omega}$ are the mass, inertia, center of mass, velocity of the center of mass and angular velocity of the rigid body B , respectively. The gravity is pointed downward in the direction of z .

To solve numerically the coupled problem (1)–(10), we have applied a distributed Lagrange multiplier-based fictitious domain method. Its basic idea is to imagine that the fluid fills the space inside as well as outside the particle boundaries. The fluid flow problem is then posed on a larger domain \mathbf{D} , the “fictitious domain”. The fictitious domain has a simple shape, allowing a simple regular mesh to be used. This domain is also time-independent, so the same mesh can be used for the entire simulation. This is a great advantage, since for simulating 3D interaction of fluid and particles, the automatic generation of unstructured boundary-fitted meshes for a large number of closely spaced particles considered in this paper is a difficult problem. The fluid inside the particle boundary must exhibit a rigid body motion of the particle. This constraint is enforced using a distributed Lagrange multiplier, which represents the additional body force per unit volume needed to maintain the rigid body motion inside the particle boundary, much like the pressure in incompressible fluid flow, whose gradient is the force required to maintain the constraint of incompressibility. For space discretization, we have used P_1 -iso- P_2 and P_1 finite elements for the velocity field and pressure, respectively (e.g., see [16, 19]). In time advancing, via the Lie's scheme [20] with the finite element approximation, the distributed Lagrange multiplier-based fictitious domain formulation of problem (1)–(10) is decoupled into a sequence of simpler subproblems at each time step and solved numerically (please see [19] for details).

3 Numerical experiments and discussion

3.1 The combined effect of the rotating rate and the number of particles

To reproduce and investigate the circular band formation similar to those observed in experiments [9, 10] for the suspensions of particles in a fully filled horizontally rotating cylinder, we have considered the cases of 16, 24, 32, and 64 balls of radius $a = 0.075$ cm and density $\rho_p = 1.25$ g/cm³ in a truncated cylinder of diameter $2R = 1$ cm and length 4 cm filled with a fluid of the density 1 g/cm³ and kinetic

viscosity $\nu = 0.15 \text{ cm}^2/\text{sec}$. The initial positions of the ball mass centers are on the circles of radius 0.35 cm centered at the central axis of the cylinder with eight balls in each circle (see Figures 2-5). We have perturbed each mass center randomly in the direction of the cylinder axis to break the symmetry of the initial pattern. The distance between two neighboring circles is about $2.25a$ hence the initial gap size d_g between balls in the cylinder axis direction is about $a/4$. In the simulations, the cylinder rotates about the cylinder axis parallel to the y -axis in a clockwise direction with rotating rate Ω equal to either 8 or 12 sec^{-1} (see Figure 1). Then the associated values of Reynolds number, $Re_p = 2aR\Omega/\nu$, are 4 and 6, respectively.

The histories of the y -coordinates of the particle mass centers and the positions of 16 balls at $t = 40$ second obtained with the rotating rates of $\Omega = 8$ and 12 sec^{-1} in Figures 2 and 6 clearly show that the 16 balls spread out in the cylinder axis direction and do not form a compact circular band at all. For the cases of 24 balls, the formation of the circular band is still not clear yet. In Figures 3 and 6, the 24 balls spread out in the cylinder axis direction at the rotating rate $\Omega = 8 \text{ sec}^{-1}$. When the rotating rate is 12 sec^{-1} , the 24 balls do form a loosely circular band. For the cases of 32 balls, the formation of the circular band is clearly shown in Figures 4 and 6. The one obtained at the rotating rate $\Omega = 12 \text{ sec}^{-1}$ is very compact. When having 64 balls, they split into two loosely circular bands at $\Omega = 8 \text{ sec}^{-1}$ since the rotating rate is not fast enough to produce strong particle interaction to sustain the whole group of particles as shown in Figures 5 and 6. But at the rotating rate $\Omega = 12 \text{ sec}^{-1}$, there is just one compact circular band and the particles are well organized in the middle of the group by the pushing from the outer particles. The particles form a layer inside the cylinder which is different from those observed in [4, 5, 6, 7], but close to those in [9, 10]. These results give us a simple observation which is that there is a need of enough particles so that the particles within a circular band can continuously interact among themselves. For the cases of 64 particles shown in Figures 5 and 9, there are 33 and 31 particles in two bands, respectively, in Figure 6 and 29 and 35 in two bands, respectively, in Figure 11. We believe that about 30 particles are enough to form a circular band for the conditions considered in this paper.

By observing the trajectories of 32 balls in Figure 7, we have found that the ball trajectories become closer to each other when the balls move downward at the back of the cylinder ($x = 0$) and they loose up (spreading out in the cylinder axis direction) when the balls move upward at the front of the cylinder ($x = 1$). A typical hydrodynamical interaction between balls called the drafting, kissing and tumbling phenomenon (e.g., see [21]), due to the fluid flow inertia, plays a role here in a fully filled horizontally rotating cylinder. When a circular band is forming, the part of a circular band formed by the balls moving downward becomes more compact due to the effects of the speedup caused by the gravity and the hydrodynamical interaction between balls. For the part of a circular band formed by the balls moving upward, it is loosening up due to the slow down of the particle motion by the counter effect of the gravity and its width becomes wider (see Figure 7). Also due to these effects of the speedup and slow down, the histories of the y -coordinates of the particle mass centers in Figure 6 show oscillations. To have a stabilized and compact circular band, enough number of balls and a fast rotating rate are needed in order to balance both effects, e.g., the results of the 32 ball cases in Figures 4 and 7 show that at the rotating rate $\Omega = 8 \text{ sec}^{-1}$, the particle speeds are not fast enough to overcome the diffusion caused by the gravity when they move upward at the front of the cylinder. But at the rotating rate $\Omega = 12 \text{ sec}^{-1}$, the particle speeds are fast enough so that a compact circular band is formed. Similarly for the 64 ball case at the rotating rate $\Omega = 8 \text{ sec}^{-1}$ in Figures 5 and 6, the particle interaction can only hold particles in two loosely circular bands; but at $\Omega = 12 \text{ sec}^{-1}$ the particle interaction can pull all 64 particles together in one compact circular band.

3.2 The effect of the band formation on the fluid flow field

In [10], Seiden et al. suggested that the formation of circular bands (e.g., in Figure 13 in [10]) is resulted by mutual interaction between the particles and the periodic inertial waves in the cylinder axis direction. Via investigating the flow field associated from the results obtained in the previous subsection, we have different point of view concerning the formation of circular bands involving the periodic inertial waves in the cylinder axis direction. The initial positions of the particles in numerical

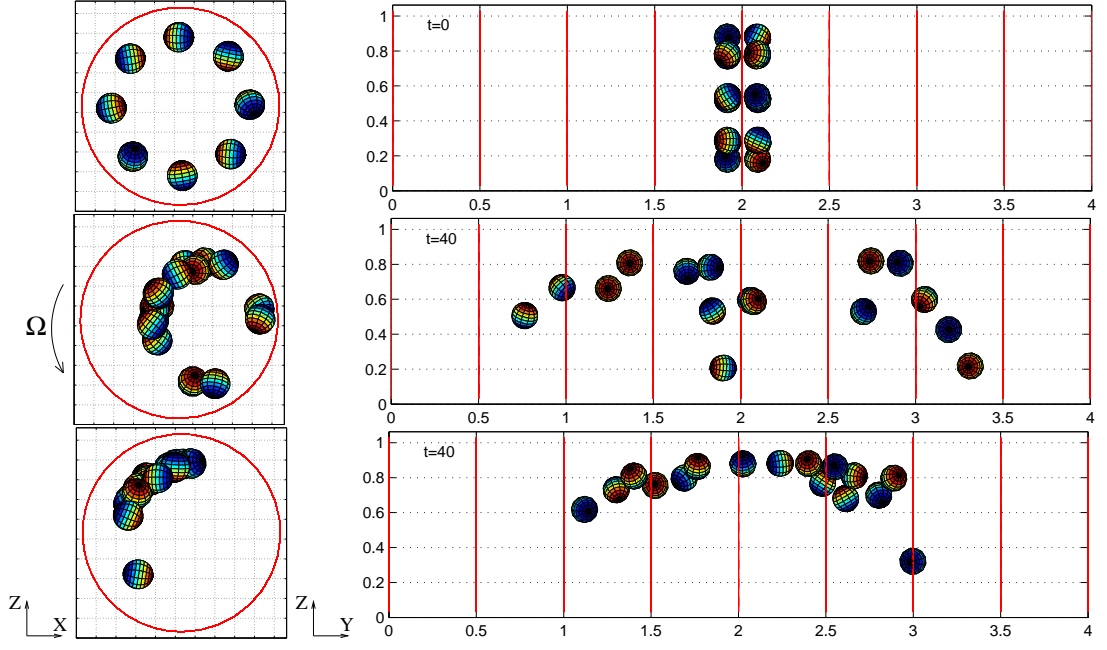


Figure 2: The side view (left) and the front view (right) of the 16 ball initial position (top) and the position obtained at the rotating rate $\Omega = 8$ (middle) and 12 (bottom) sec^{-1} at $t = 40$ second.

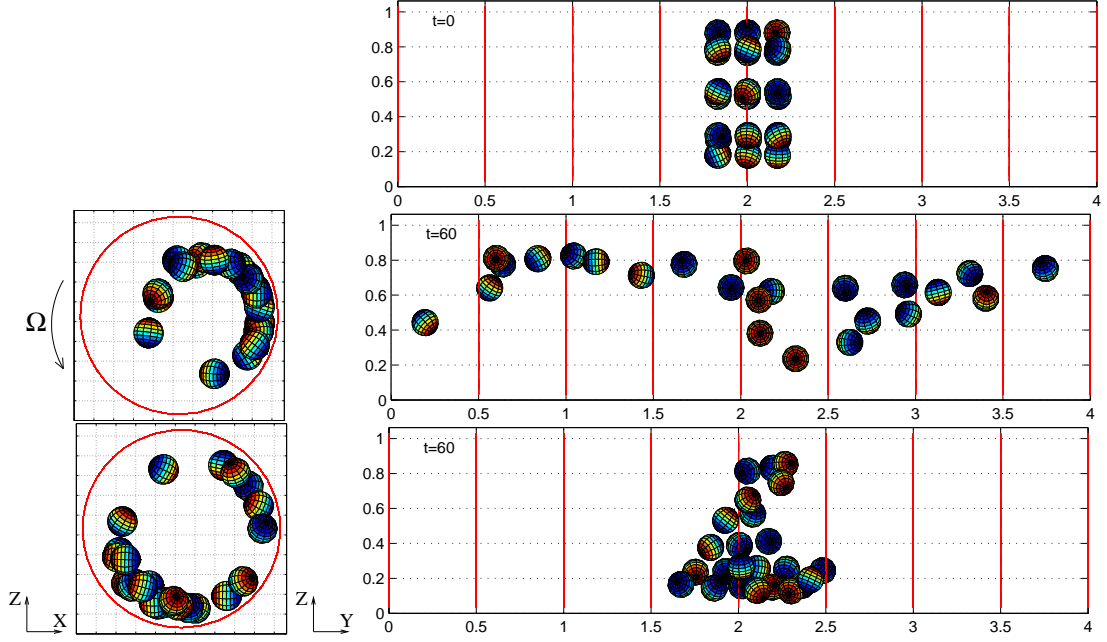


Figure 3: The side view (left) and the front view (right) of the 24 ball initial position (top) and the position obtained at the rotating rate $\Omega = 8$ (middle) and 12 (bottom) sec^{-1} at $t = 60$ second.

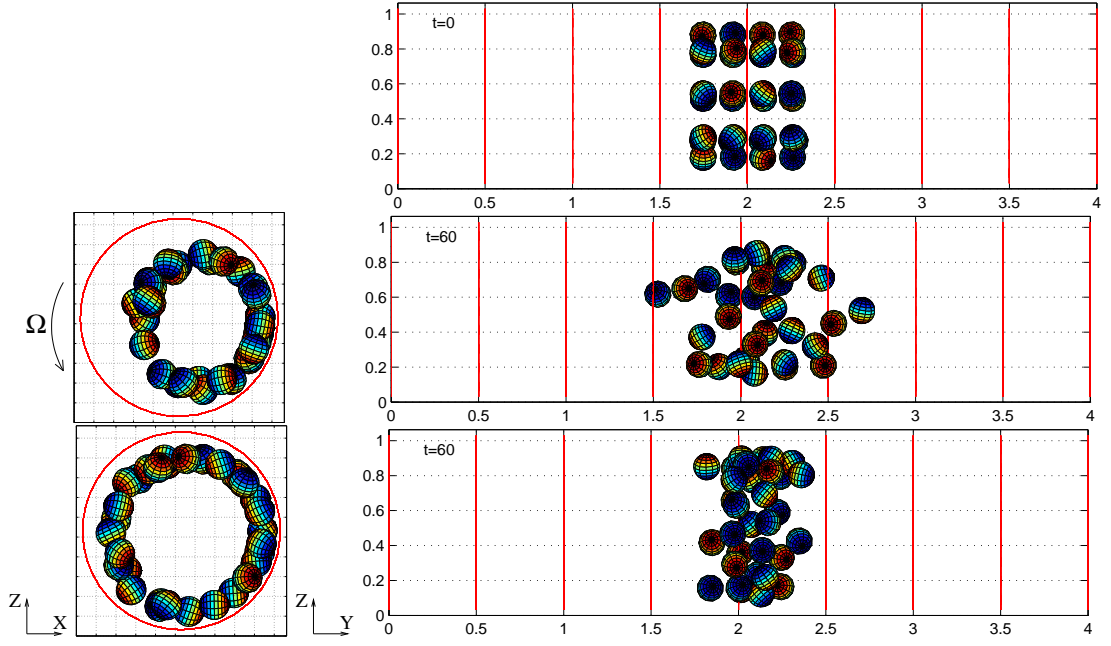


Figure 4: The side view (left) and the front view (right) of the 32 ball initial position (top) and the position obtained at the rotating rate $\Omega = 8$ (middle) and 12 (bottom) sec^{-1} at $t = 60$ second.

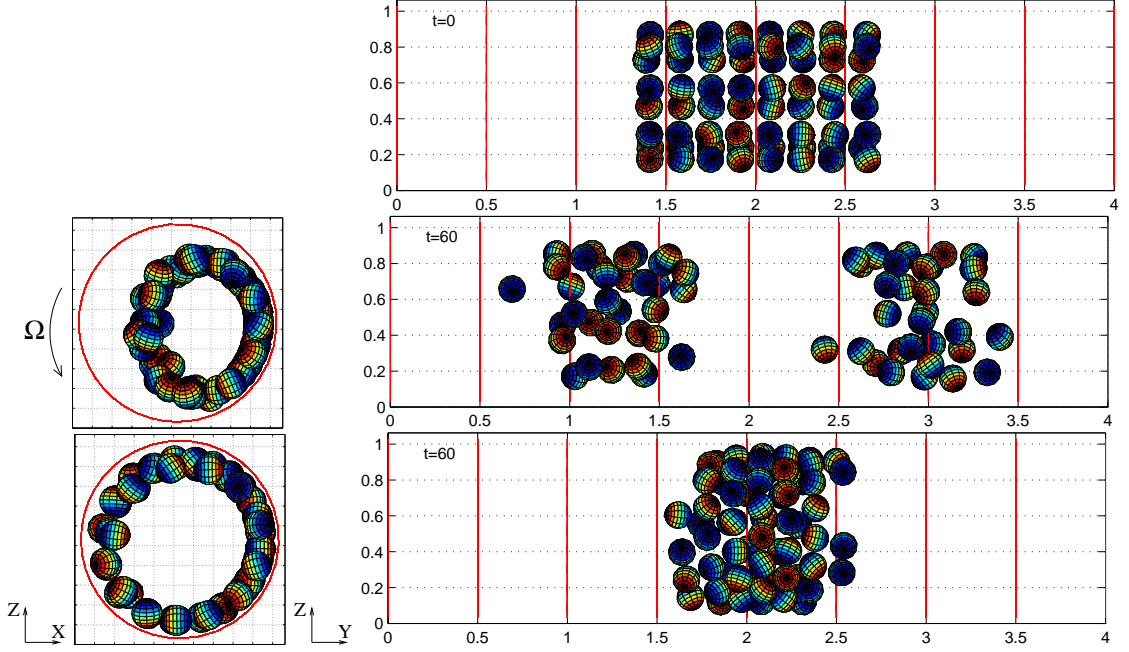


Figure 5: The side view (left) and the front view (right) of the 64 ball initial position (top) and the position obtained at the rotating rate $\Omega = 8$ (middle) and 12 (bottom) sec^{-1} at $t = 60$ second.

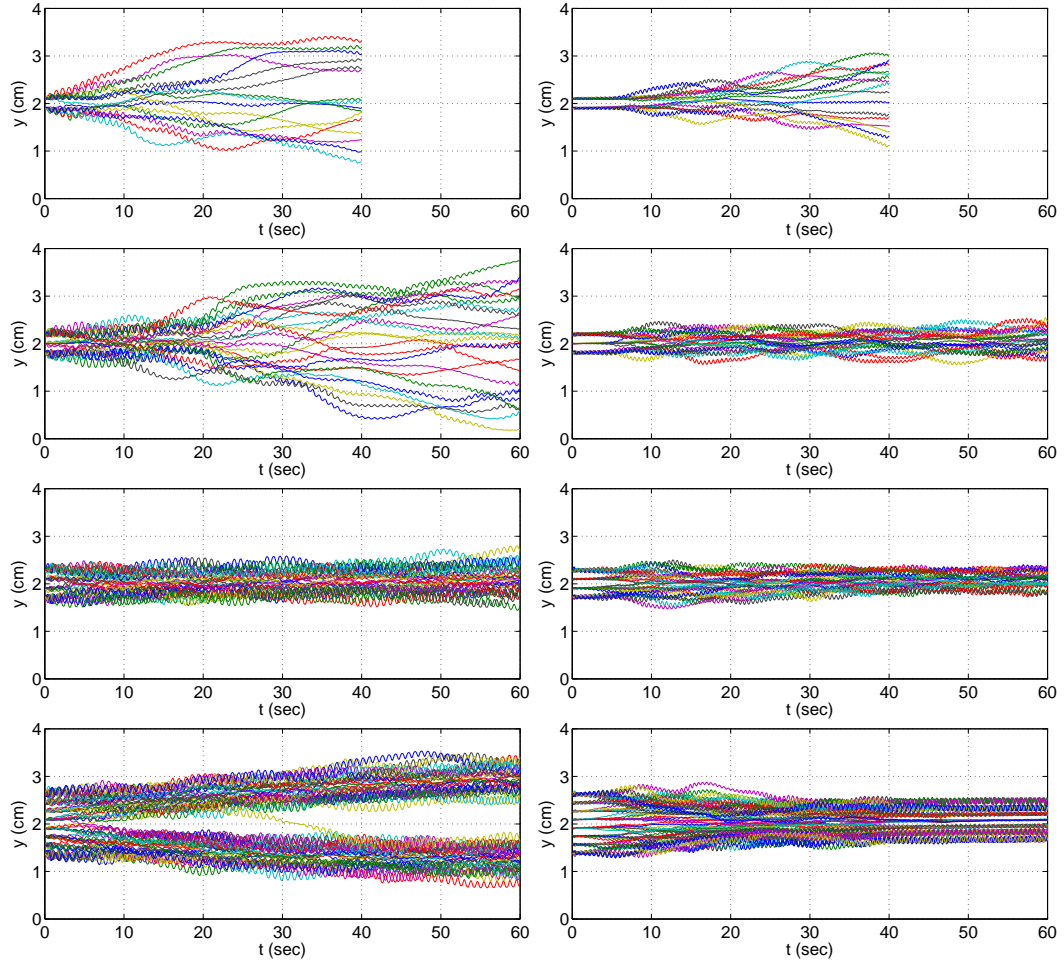


Figure 6: The histories of the y -coordinates of the mass centers of 16, 24, 32, and 64 balls (from top to bottom): $\Omega = 8$ (left) and 12 (right) sec^{-1} .

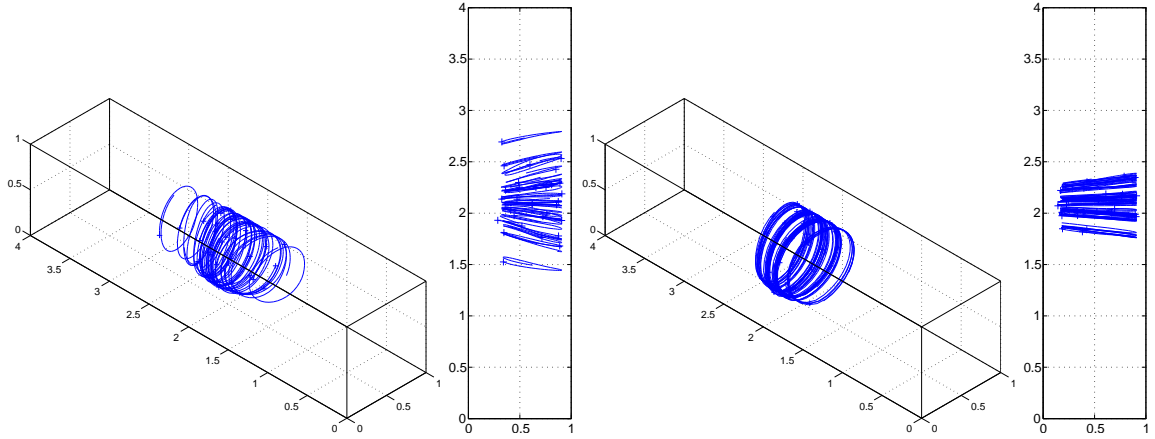


Figure 7: The trajectories and the top view of the trajectories of the 32 balls at the rotating rate $\Omega = 8$ (left two) and 12 (right two) sec^{-1} for $59 \leq t \leq 60$.

simulations are not easy to set up experimentally; but such kind of arrangement does help us to understand the formation of circular bands. For the case of 32 balls and $\Omega = 12 \text{ sec}^{-1}$ studied in the previous subsection, the projections of the velocity field on the vertical plane passing through the central axis of the cylinder at different time are shown in Figure 8. The 32 particles do not excite the entire flow field inside the rotating cylinder into a periodic flow field in the cylinder axis direction at all. The circulation of the velocity field is created only by the particle motion and concentrated in the middle portion of the cylinder. For the evolution of the flow field related to two circular bands, the results of the case of 64 balls with the initial gap size $d_g = 2a$ and the rotating rate $\Omega = 12 \text{ sec}^{-1}$ are shown in Figures 9 and 11. We have observed no periodic flow field from the beginning as in Figure 9. The particles break into two circular bands between $t = 16$ and 19 second and then two bands move away from each other as in Figure 11 and the projected velocity fields at $t = 19$ and 100 second in Figure 9 show that the two circulations move apart since the two circular bands move away from each other. The projected velocity field at $t = 100$ second in Figure 9 is similar to the one in Figure 13 in [10] obtained experimentally in [10], but the circulation of the flow field is caused by the motion of the particles in the two circular particle bands. Similarly for the case of 128 balls in a truncated cylinder of length $L = 8 \text{ cm}$ at the rotating rate $\Omega = 12 \text{ sec}^{-1}$ with the initial gap size $d_g = a/4$, the particles are initially placed on 16 circles in the middle of the cylinder as in the previous subsection. Later they break into two compact circular bands as shown in Figures 10 and 11. There are 63 and 65 particles in these two circular bands, respectively, which are consistent with the results of the 64 particles at the rotating rate $\Omega = 12 \text{ sec}^{-1}$ discussed in the previous subsection. The figures of the circulation of the flow field at $t = 6$ and 40 second in Figure 10 clearly show that there is no periodic flow field pattern in the cylinder axis direction, but there is only one large circulation at the beginning and then two circulations are created by the two particle bands once the particles break into two groups.

To reproduce the circular bands similar to the one in Figure 5 in [10], we have considered the case of 128 balls in a truncated cylinder of length $L = 4 \text{ cm}$. We have first placed 128 balls on 16 circles in the middle of the cylinder with the initial gap size $d_g = a/4$ as in the previous subsection and then let them settle at the zero rotating rate. The particles are down to the bottom of the cylinder after 2 seconds as shown in Figure 12. Then we rotate the cylinder at the rate $\Omega = 12 \text{ sec}^{-1}$. Those 128 particles first move up and down inside the rotating cylinder and interact with the fluid. At $t = 5$ second, there is no periodic flow field pattern in the cylinder axis direction. About $t = 20$ second, two outer bands next to the two ends of the cylinder start forming. Gradually three circular bands, which are similar to the one obtained experimentally in Figure 5 in [10], are formed as shown in Figure 12. All above cases show that the circular bands cause the flow field circulations, at least, for the cases considered in the paper.

4 Conclusion

In this article we have applied a distributed Lagrange multiplier fictitious domain method to simulate rotating suspension of particles and to study the interaction between balls and fluid in a fully filled and horizontally rotating cylinder. The formation of circular bands studied in this paper is not resulted by mutual interaction between the particles and the periodic inertial waves in the cylinder axis direction, but as the result of the interaction of particles. When a circular band is forming, the part of the band formed by the particles moving downward becomes more compact due to the particle interaction strengthened by the downward acceleration from the gravity. The part of a band formed by the particles moving upward is always loosening up due to the slow down of the particle motion by the counter effect of the gravity. To form a compact circular band (not a loosely one), enough particles are needed to have continuous interaction among themselves through the entire circular band at a rotating rate so that the upward diffusion of particles can be overcome by the compactness process when these particles moving downward. Hence the balance of the gravity, the rotating rate, and the fluid flow inertia and the number of particles are important on the formation of circular bands.

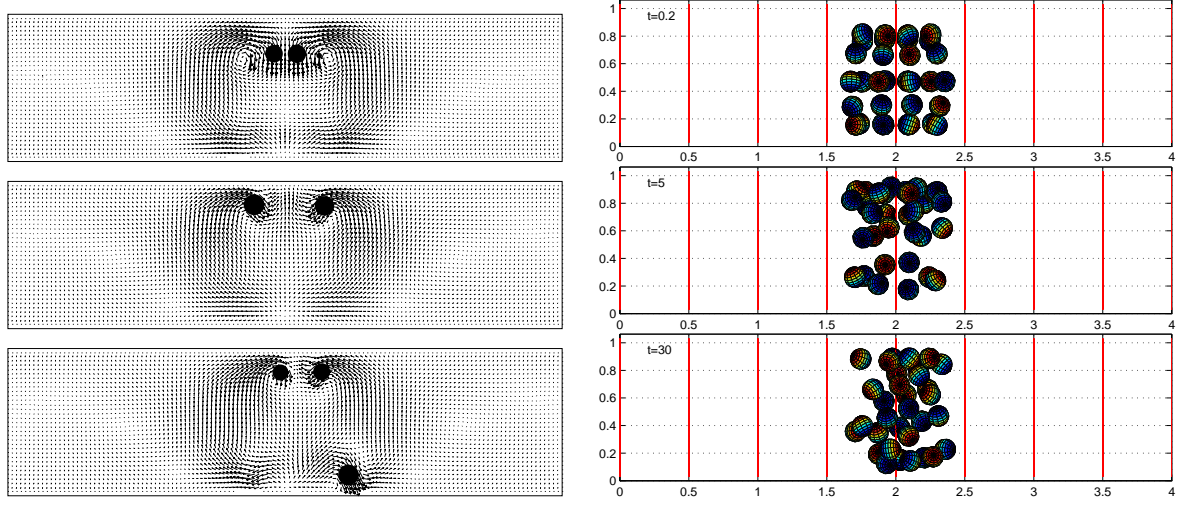


Figure 8: (a) The projection of the velocity field on the vertical plane passing through the central axis of the cylinder for the case of 32 balls (left) and (b) the front view of the position of 32 balls (right) at $t = 0.2, 5$ and 30 second (from top to bottom) with $\Omega = 12 \text{ sec}^{-1}$.

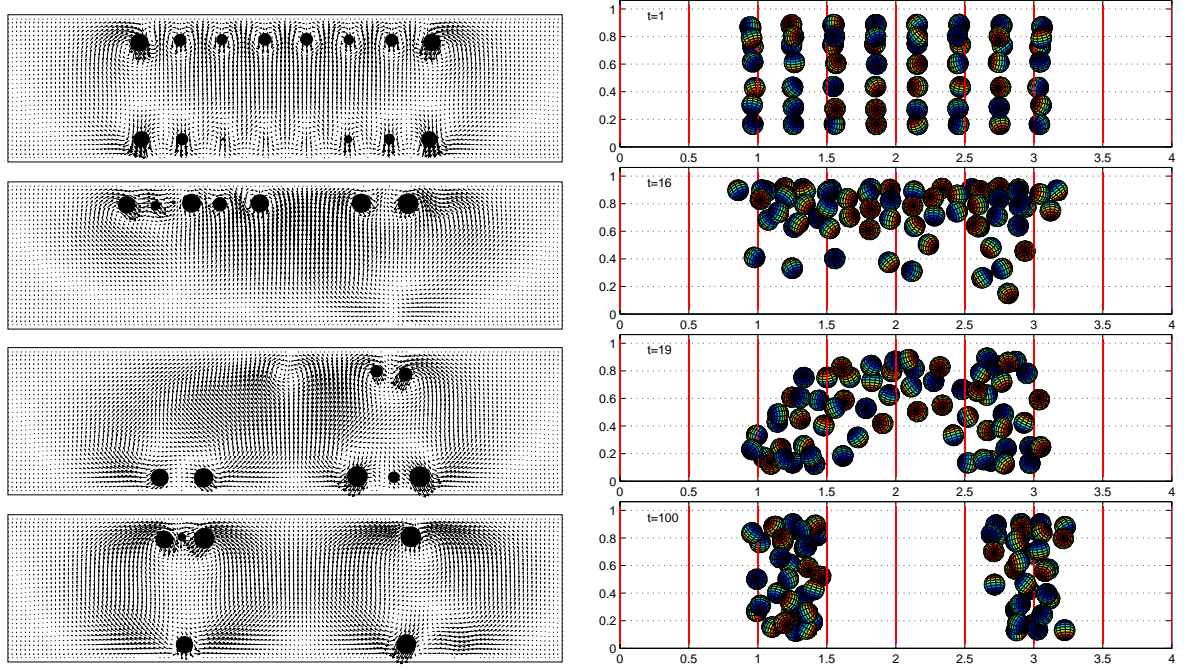


Figure 9: (a) The projection of the velocity field on the vertical plane passing through the central axis of the cylinder for the case of 64 balls (left) and (b) the front view of the position of 64 balls (right) at $t = 1, 16, 19$ and 100 second (from top to bottom) with $\Omega = 12 \text{ sec}^{-1}$ and the initial gap size $d_g = 2a$.

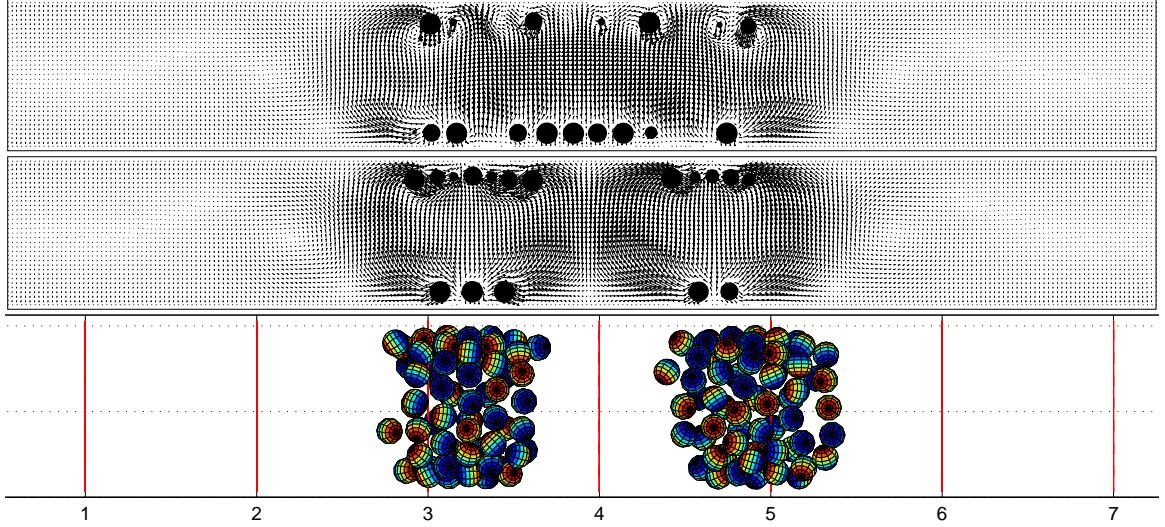


Figure 10: The projection of the velocity field on the vertical plane passing through the central axis of the cylinder for the case of 128 balls at $t = 6$ (top) and 40 second (middle) and the front view of the position of 128 balls (bottom) at $t = 40$ second.

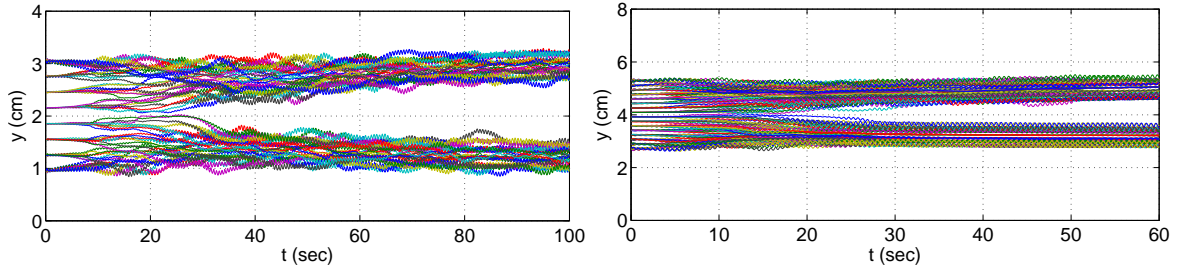


Figure 11: The histories of the y -coordinates of the mass centers of 64 balls with the initial gap size $d_g = 2a$ (left) and 128 balls with the initial gap size $d_g = a/4$ (right).

Acknowledgments

The authors acknowledge the helpful comments and suggestions of Howard H. Hu and Penger Tong. T.W. Pan and R. Glowinski acknowledge the support of NSF (grant DMS-0914788).

References

- [1] M. Tirumkudulu, A. Tripathi, and A. Acrivos, Phys. Fluids **11**, S13 (1999).
- [2] M. Tirumkudulu, A. Mileo, and A. Acrivos, Phys. Fluids **12**, 1615 (2000).
- [3] D. D. Joseph, J. Wang, R. Bai, B. H. Yang, and H. H. Hu, J. Fluid Mech. **496**, 139 (2003).
- [4] W. R. Matson, B. J. Ackerson, and P. Tong, Phys. Rev. E **67**, 050301 (2003).
- [5] W. P. Matson, M. Kalyankar, B. J. Ackerson, and P. Tong, Phys. Rev. E **71**, 031401 (2005).
- [6] W. R. Matson, B. J. Ackerson, B. J. and P. Tong, J. Fluid Mech. **597**, 233 (2008).

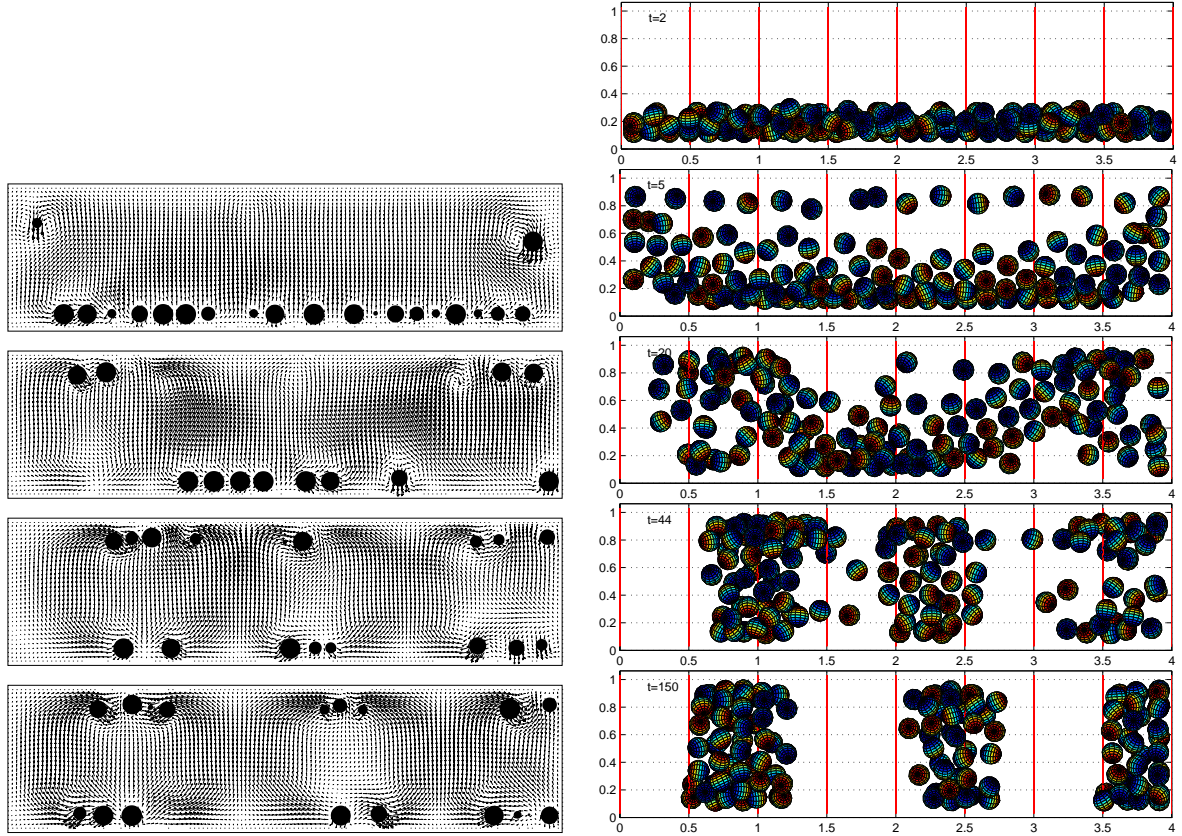


Figure 12: (a) The projection of the velocity field on the vertical plane passing through the central axis of the cylinder for the case of 128 balls (left) and (b) the front view of the position of 128 balls (right) at $t = 2, 5, 44, 20$ and 150 second (from top to bottom) with $\Omega = 12 \text{ sec}^{-1}$.

- [7] A. P. J. Breu, C. A. Kruelle, and I. Rehberg, *Europhys. Lett.* **62**, 491 (2003).
- [8] S. G. Lipson, *J. Phys.: Condens. Matters* **13**, 5001 (2001).
- [9] S. G. Lipson and G. Seiden *Physica A* **314**, 272 (2002).
- [10] G. Seiden, M. Ungarish, and S. G. Lipson, *Phys. Rev. E* **72**, 021407 (2005).
- [11] J. H. Lee and A. J. C. Ladd, *Phys. Rev. Lett.* **95**, 048001 (2005).
- [12] J. H. Lee and A. J. C. Ladd, *J. Fluid Mech.* **577**, 183 (2007).
- [13] G. Seiden, M. Ungarish, and S. G. Lipson, *Phys. Rev. E* **76**, 026221 (2007).
- [14] R. Glowinski, T.-W. Pan, T. Hesla, and D. D. Joseph, *Int. J. Multiphase Flow* **25**, 755 (1999).
- [15] R. Glowinski, T.-W. Pan, T. Hesla, D. D. Joseph, and J. Periaux, *J. Comput. Phys.* **169**, 363 (2001).
- [16] R. Glowinski, *Finite element methods for incompressible viscous flow* (Handbook of Numerical Analysis, Vol. IX (Ciarlet PG, Lions JL, editors) North-Holland, Amsterdam, 2003).
- [17] T.-W. Pan, D. D. Joseph, R. Bai, R. Glowinski, and V. Sarin, *J. Fluid Mech.* **451**, 169 (2002).
- [18] B. H. Yang, J. Wang, D. D. Joseph, H. H. Hu, T.-W. Pan, and R. Glowinski, *J. Fluid Mech.* **540**, 109 (2005).

- [19] T.-W. Pan, R. Glowinski, and S. C. Hou, Computers and Structures **85**, 955 (2007).
- [20] A. J. Chorin, T. J. R. Hughes, J. E. Marsden, and M. McCracken, Comm. Pure Appl. Math. **31**, 205 (1978).
- [21] A. F. Fortes, D. D. Joseph, and T. S. Lundgren, J. Fluid Mech. **177**, 467 (1987)